ICHEP94 Ref. GLS0159 **CLEO CONF 94-2**
Submitted to PA 21,2 Pl 9,19

A Constraint on $|V_{td}/V_{ts}|$ from $B \to \rho(\omega)\gamma/B \to K^*\gamma$.

M. Athanas,[1] W. Brower,[1] G. Masek,[1] H.P. Paar,[1] J. Gronberg,[2] R. Kutschke,[2] S. Menary,[2] R.J. Morrison,[2] S. Nakanishi,[2] H.N. Nelson,[2] T.K. Nelson,[2] C. Qiao,[2] J.D. Richman,[2] A. Ryd,[2] H. Tajima,[2] D. Sperka,[2] M.S. Witherell,[2] R. Balest,[3] K. Cho,[3] W.T. Ford,[3] D.R. Johnson,[3] K. Lingel,[3] M. Lohner,[3] P. Rankin,[3] J.G. Smith,[3] J.P. Alexander,[4] C. Bebek,[4] K. Berkelman,[4] K. Bloom,[4] T.E. Browder,[4*] D.G. Cassel,[4] H.A. Cho,[4] D.M. Coffman,[4] D.S. Crowcroft,[4] P.S. Drell,[4] D. Dumas,[4] R. Ehrlich,[4] P. Gaidarev,[4] M. Garcia-Sciveres,[4] B. Geiser,[4] B. Gittelman,[4] S.W. Gray,[4] D.L. Hartill,[4] B.K. Heltsley,[4] S. Henderson,[4] C.D. Jones,[4] S.L. Jones,[4] J. Kandaswamy,[4] N. Katayama,[4] P.C. Kim,[4] D.L. Kreinick,[4] G.S. Ludwig,[4] J. Masui,[4] J. Mevissen,[4] N.B. Mistry,[4] C.R. Ng,[4] E. Nordberg,[4] J.R. Patterson,[4] D. Peterson,[4] D. Riley,[4] S. Salman,[4] M. Sapper,[4] F. Würthwein,[4] P. Avery,[5] A. Freyberger,[5] J. Rodriguez,[5] S. Yang,[5] J. Yelton,[5] D. Cinabro,[6] T. Liu,[6] M. Saulnier,[6] R. Wilson,[6] H. Yamamoto,[6] T. Bergfeld,[7] B.I. Eisenstein,[7] G. Gollin,[7] B. Ong,[7] M. Palmer,[7] M. Selen,[7] J. J. Thaler,[7] K.W. Edwards,[8] M. Ogg,[8] A. Bellerive,[9] D.I. Britton,[9] E.R.F. Hyatt,[9] D.B. MacFarlane,[9] P.M. Patel,[9] B. Spaan,[9] A.J. Sadoff,[10] R. Ammar,[11] P. Baringer,[11] A. Bean,[11] D. Besson,[11] D. Coppage,[11] N. Copty,[11] R. Davis,[11] N. Hancock,[11] M. Kelly,[11] S. Kotov,[11] I. Kravchenko,[11] N. Kwak,[11] H. Lam,[11] Y. Kubota,[12] M. Lattery,[12] M. Momayezi,[12] J.K. Nelson,[12] S. Patton,[12] R. Poling,[12] V. Savinov,[12] S. Schrenk,[12] R. Wang,[12] M.S. Alam,[13] I.J. Kim,[13] Z. Ling,[13] A.H. Mahmood,[13] J.J. O'Neill,[13] H. Severini,[13] C.R. Sun,[13] F. Wappler,[13] G. Crawford,[14] C. M. Daubenmier,[14] R. Fulton,[14] D. Fujino,[14] K.K. Gan,[14] K. Honscheid,[14] H. Kagan,[14] R. Kass,[14] J. Lee,[14] R. Malchow,[14] Y. Skovpen,[14†] M. Sung,[14] C. White,[14] M.M. Zoeller,[14] F. Butler,[15] X. Fu,[15] B. Nemati,[15] W.R. Ross,[15] P. Skubic,[15] M. Wood,[15] M. Bishai,[16] J. Fast,[16] E. Gerndt,[16] R.L. McIlwain,[16] T. Miao,[16] D.H. Miller,[16] M. Modesitt,[16] D. Payne,[16] E.I. Shibata,[16] I.P.J. Shipsey,[16] P.N. Wang,[16] M. Battle,[17] J. Ernst,[17] L. Gibbons,[17] Y. Kwon,[17] S. Roberts,[17] E.H. Thorndike,[17] C.H. Wang,[17] J. Dominick,[18] M. Lambrecht,[18] S. Sanghera,[18] V. Shelkov,[18] T. Skwarnicki,[18] R. Stroynowski,[18] I. Volobouev,[18] G. Wei,[18] P. Zadorozhny,[18] M. Artuso,[19] M. Gao,[19] M. Goldberg,[19] D. He,[19] N. Horwitz,[19] R. Kennett,[19] R. Mountain,[19] G.C. Moneti,[19] F. Muheim,[19] Y. Mukhin,[19] S. Playfer,[19] Y. Rozen,[19] S. Stone,[19] X. Xing,[19] G. Zhu,[19] J. Bartelt,[20] S.E. Csorna,[20] Z. Egyed,[20] V. Jain,[20] D. Gibaut,[21] K. Kinoshita,[21] P. Pomianowski,[21] B. Barish,[22] M. Chadha,[22] S. Chan,[22] D.F. Cowen,[22] G. Eigen,[22] J.S. Miller,[22] C. O'Grady,[22] J. Urheim,[22] and A.J. Weinstein[22]

(CLEO Collaboration)

[1] *University of California, San Diego, La Jolla, California 92093*
[2] *University of California, Santa Barbara, California 93106*
[3] *University of Colorado, Boulder, Colorado 80309-0390*
[4] *Cornell University, Ithaca, New York 14853*
[5] *University of Florida, Gainesville, Florida 32611*
[6] *Harvard University, Cambridge, Massachusetts 02138*
[7] *University of Illinois, Champaign-Urbana, Illinois, 61801*
[8] *Carleton University, Ottawa, Ontario K1S 5B6 and the Institute of Particle Physics, Canada*
[9] *McGill University, Montréal, Québec H3A 2T8 and the Institute of Particle Physics, Canada*
[10] *Ithaca College, Ithaca, New York 14850*
[11] *University of Kansas, Lawrence, Kansas 66045*
[12] *University of Minnesota, Minneapolis, Minnesota 55455*
[13] *State University of New York at Albany, Albany, New York 12222*
[14] *Ohio State University, Columbus, Ohio, 43210*
[15] *University of Oklahoma, Norman, Oklahoma 73019*
[16] *Purdue University, West Lafayette, Indiana 47907*
[17] *University of Rochester, Rochester, New York 14627*
[18] *Southern Methodist University, Dallas, Texas 75275*
[19] *Syracuse University, Syracuse, New York 13244*
[20] *Vanderbilt University, Nashville, Tennessee 37235*
[21] *Virginia Polytechnic Institute and State University, Blacksburg, Virginia, 24061*
[22] *California Institute of Technology, Pasadena, California 91125*

Abstract

We have searched for the decays, $B \to \rho\gamma$ and $B \to \omega\gamma$, which in conjunction with the measurement of $B \to K^*\gamma$, can provide a direct determination of the ratio between the CKM matrix elements, V_{td} and V_{ts}. No signals were observed and we set the following upper limits (90% CL): $\mathcal{B}(B^- \to \rho^-\gamma) < 2.0 \times 10^{-5}$, $\mathcal{B}(\bar{B}^0 \to \rho^0\gamma) < 2.4 \times 10^{-5}$, and $\mathcal{B}(\bar{B}^0 \to \omega\gamma) < 1.1 \times 10^{-5}$. Using different theoretical models, we also set a range of upper limits on $|V_{td}/V_{ts}| < 0.64 - 0.76$.

*Permanent address: University of Hawaii at Manoa

†Permanent address: INP, Novosibirsk, Russia

Last year CLEO reported the first observation of $B \to K^*\gamma$, a flavor-changing neutral current (FCNC) penguin diagram decay [1]. This paper describes a search for three related FCNC penguin decays, $B^- \to \rho^-\gamma$, $\bar{B}^0 \to \omega\gamma$, and $\bar{B}^0 \to \rho^0\gamma$ mediated by the quark level process $b \to d\gamma$. The Feynman diagrams associated with these decays are shown in Figure 1. The diagram with the top quark in the loop is the dominant short distance contribution to the amplitude. Exclusive $b \to s\gamma$ decays are proportional to $|V_{ts}|^2$ while the corresponding $b \to d\gamma$ decays are proportional to $|V_{td}|^2$. Long distance effects are expected to be negligible for both the $K^*\gamma$ and $\rho(\omega)\gamma$ decays [2]. Therefore one can extract the ratio $|V_{td}/V_{ts}|$ from

$$\frac{\mathcal{B}(B^- \to \rho^-\gamma)}{\mathcal{B}(B^- \to K^{*-}\gamma)} = \frac{\mathcal{B}(\bar{B}^0 \to \omega\gamma) + \mathcal{B}(\bar{B}^0 \to \rho^0\gamma)}{\mathcal{B}(\bar{B}^0 \to \bar{K}^{*0}\gamma)} = \left|\frac{V_{td}}{V_{ts}}\right|^2 \xi\Omega \tag{1}$$

where Ω is a small correction for phase space and ξ accounts for the SU(3) symmetry breaking. The factor ξ is model dependent and is predicted to lie in the range $0.58 - 0.81$. Uncertainties due to the top quark mass and QCD corrections cancel in this ratio.

The data sample used in this study was collected with the CLEO-II detector at the Cornell Electron Storage Ring (CESR). It consists of 2040 pb^{-1} of integrated luminosity on the $\Upsilon(4S)$ resonance (2.19×10^6 $B\bar{B}$ events) and 967 pb^{-1} taken at a center of mass energy 55 MeV below the resonance. Charged particles are tracked using three nested cylindrical wire chambers operated in a 1.5T magnetic field. The outer tracking chamber also measures specific ionization (dE/dx), which is used for particle identification. The tracking chambers are followed by time-of-flight (TOF) scintillation counters, which provide additional particle identification information. Beyond the TOF system but still inside the superconducting magnetic coil is an electromagnetic calorimeter consisting of 7800 CsI crystals. Outside the coil is an iron yoke for field return, with chambers interspersed for muon identification.

The three decay modes, $\bar{B}^0 \to \omega\gamma$, $\omega \to \pi^-\pi^+\pi^0$; $\bar{B}^0 \to \rho^0\gamma$, $\rho^0 \to \pi^-\pi^+$; and $B^- \to \rho^-\gamma$, $\rho^- \to \pi^-\pi^0$ use event selection criterion very similar to the previous $\bar{B}^0 \to \bar{K}^{*0}\gamma$ analysis. We select events with at least 3 charged tracks and a measured energy of at least 30% of the center-of-mass energy. High energy photon candidates are showers in the calorimeter with $2.0 < E_\gamma < 3.0$ GeV. In addition, the photon candidates must not be matched to a charged track, must have a polar angle θ (relative to the beam axis) satisfying $|\cos\theta| < 0.7$, and must have a shower shape consistent with a single photon. Photon candidates are rejected if they form π^0's (η's) when combined with another photon of energy greater than 30 (200) MeV.

The charged tracks must pass standard track quality cuts, and must have a measured ionization loss (dE/dx) or TOF within 2.5 standard deviations (σ) of that expected for the mass hypothesis. Particles lacking both TOF and dE/dx measurements are considered as pion candidates only. Candidate π^0 mesons are reconstructed from pairs of electromagnetic showers which are not matched to any charged tracks. Each shower must have $E_\gamma > 30$ MeV if the polar angle satisfies $|\cos\theta| < 0.7$ or $E_\gamma > 50$ MeV if $0.7 < |\cos\theta| < 0.95$. To suppress combinatorial background, the invariant mass of the pair must lie between 120 and 150 MeV and satisfy a minimum momentum requirement that is mode dependent ($P_{\gamma\gamma} > 1.0$ GeV for $B^- \to \rho^-\gamma$ and $P_{\gamma\gamma} > 0.25$ GeV for $\bar{B}^0 \to \omega\gamma$).

When forming ρ or ω candidates, decay angle and invariant mass cuts are used. For ρ candidates the decay angle, θ_{decay}, is the angle between the flight direction of the ρ in the lab frame and the flight direction of a charged daughter in the ρ's rest frame. For ω

candidates the decay angle is the angle between the ω's flight direction in the lab frame, and the normal to the plane defined by the three daughters in the ω's rest frame. For ρ^-, ρ^0, and ω candidates, a decay angle cut of $|\cos\theta_{decay}| < 0.8$ is used since all decay according to a $\sin^2\theta_{decay}$ distribution, whereas the background is nearly flat with some peaking at 1.0. Candidate $\omega \to \pi^-\pi^+\pi^0$ decays must have an invariant mass which satisfies $740 < M_{(\pi^-\pi^+\pi^0)} < 820$ MeV. Candidate ρ^- and ρ^0 mesons must satisfy $619 < M_{\pi\pi} < 921$ MeV.

The dominant background to these radiative penguin decays arises from continuum (non-$B\bar{B}$) processes. There are two main sources of high energy photons from the continuum: initial state radiation (ISR) and fragmentation of non-$b\bar{b}$ quarks ($q\bar{q}$). We suppress this background with a series of cuts determined from Monte Carlo (MC) studies. Most continuum processes have a two-jet topology. By contrast, pairs of B mesons are produced nearly at rest and decay isotropically. We suppress $q\bar{q}$ backgrounds by applying cuts on the following shape variables: the normalized second Fox-Wolfram moment [4], R_2, and a measure of the momentum transverse to the photon direction, $S_\perp$.[1] We require $R_2 < 0.5$ and $0.25 < S_\perp < 0.60$ (the upper restriction on $S_\perp$ provides rejection of ISR events). To further suppress the ISR background we use variables evaluated in the rest frame of the e^+e^- following the radiation of the high energy photon (the primed frame). In this frame we require $R_2' < 0.3$, where R_2' is evaluated excluding the photon, and $|\cos\theta'| > 0.5$, where θ' is the angle between the photon and the thrust axis of the rest of the event.

We combine the high energy photon and ρ or ω candidates to form $B \to \rho\gamma$ or $\bar{B}^0 \to \omega\gamma$ candidates. Having made all particle assignments, we impose two further cuts. The angle θ_{thr} between the high energy photon direction and the thrust axis of the particles not from the B candidate is required to satisfy $|\cos\theta_{thr}| < 0.7$. The signal distribution in $|\cos\theta_{thr}|$ is expected to be flat, while the continuum background peaks at 1.0. For the production polar angle of the B, we require $|\cos\theta_B| < 0.85$ (expected to have a $\sin^2\theta_B$ distribution for signal, flat for background). Finally, we require that B candidates have an energy close to the beam energy, $|\Delta E| < 90$ MeV (2.2σ) for $\bar{B}^0 \to \rho^0\gamma$ and $\bar{B}^0 \to \omega\gamma$ or $-150 < \Delta E < 90$ MeV for $B^- \to \rho^-\gamma$, where $\Delta E = E_B - E_{beam}$. For candidates passing this cut, we scale the photon energy to obtain $\Delta E = 0$, and compute M_B. The M_B resolution of 2.8 MeV r.m.s. is dominated by the spread in beam energy.

All of these radiative penguin decays are kinematically very similar. This similarity and the difficulty in distinguishing a K^- from a π^- in the momentum range 1.1 to 2.2 GeV where neither dE/dx nor TOF gives significant π/K separation allows for the possibility of a $B \to K^*\gamma$ event being misidentified as a $B \to \rho\gamma$ event. The $\bar{B}^0 \to \omega\gamma$ mode does not have an appreciable feed-through because the ω is a narrow resonance and the K^* cannot be misinterpreted as an ω. The $B^- \to \rho^-\gamma$ mode can only get feed-through from $B^- \to K^{*-}\gamma$, $K^{*-} \to K^-\pi^0$. This is negligible compared to the continuum background because the $K^{*-} \to K^-\pi^0$ branching fraction is only 33% and the $P_{\pi^0} > 1$ GeV cut on π^0's also rejects K^* decays. On the other hand, the $\bar{B}^0 \to \rho^0\gamma$ mode does have a significant

[1] $S_\perp$ is defined as the sum of the magnitudes of the momenta transverse to the photon direction, summed over all particles more than 45° away from the photon axis, divided by the sum of the magnitudes of the momenta of all particles except the photon.

TABLE I. Summary of results

		Events in Signal Region	Estimated background	Efficiency	Branching ratio ($\times 10^{-5}$)
$\bar{B}^0 \to \bar{K}^{*0}\gamma$	$\bar{K}^{*0} \to K^-\pi^+$	8	1.1 ± 0.2	11.9%	
$B^- \to K^{*-}\gamma$	$K^{*-} \to K^0_S\pi^-$	2	0.01 ± 0.01	2.0%	$(4.5 \pm 1.5 \pm 0.9)$
	$K^{*-} \to K^-\pi^0$	3	0.8 ± 0.3	3.1%	from Ref. [1]
$\bar{B}^0 \to \omega\gamma$	$\omega \to \pi^0\pi^+\pi^-$	0	0.8 ± 0.2	12.0%	< 1.05
$\bar{B}^0 \to \rho^0\gamma$	$\rho^0 \to \pi^+\pi^-$	1	2.2 ± 0.2	9.2%	< 2.4
$B^- \to \rho^-\gamma$	$\rho^- \to \pi^-\pi^0$	1	1.1 ± 0.2	10.6%	< 2.0

background from the mode $\bar{B}^0 \to \bar{K}^{*0}\gamma$ since the $K^{*0} \to K^-\pi^+$ branching fraction is 67% and there is less combinatorial background. With no additional cuts we would expect to see about 7 $\bar{B}^0 \to \bar{K}^{*0}\gamma$ events in the $\bar{B}^0 \to \rho^0\gamma$ signal region.

We use a neural network technique [5,6] to distinguish $\bar{B}^0 \to \rho^0\gamma$ from $\bar{B}^0 \to \bar{K}^{*0}\gamma$. The neural network produces one output, r, with values between -1 and 1, from four inputs ΔE, $M_{\pi\pi}$, $M_{K\pi}$, and $\cos\theta_{decay}$, where K is assumed to be the higher momentum track of the pair. The input distributions for $\bar{B}^0 \to \rho^0\gamma$ signal and $B \to K^*\gamma$ background are shown in Figure 2 and the output neural network variable, r, is shown in Figure 3. True $\bar{B}^0 \to \bar{K}^{*0}\gamma$ events that have been misidentified as $\bar{B}^0 \to \rho^0\gamma$ candidates have lower ΔE and momentum than true $\bar{B}^0 \to \rho^0\gamma$ events and this is reflected in their distributions in the four input variables and in a smaller value of r. Since these four kinematic quantities are reproduced well by the MC simulation, the neural network was trained with $\bar{B}^0 \to \rho^0\gamma$ and $\bar{B}^0 \to \bar{K}^{*0}\gamma$ MC events. We require $r > 0.56$, since that requirement optimizes the sensitivity, according to MC studies, for a wide range of $(\bar{B}^0 \to \rho^0\gamma/\bar{B}^0 \to \bar{K}^{*0}\gamma)$ ratios. The neural network cut retains 50% of the $\bar{B}^0 \to \rho^0\gamma$ signal and only 4.7% of the $\bar{B}^0 \to \bar{K}^{*0}\gamma$ background. The mass distribution of the B candidates for the $b \to d\gamma$ modes after all cuts is shown in Figure 4.

Table I gives the number of events seen in the signal region and the efficiency of the selection criteria for the three $b \to d\gamma$ decay channels. The results for the three $B \to K^*\gamma$ channels from Ref. [1] are also included [7]. The estimated background for the three $b \to d\gamma$ modes is determined from the data using the same method used to estimate background for the $B \to K^*\gamma$ channels. When calculating the upper limits on the three new modes, we conservatively assume all the events in the signal region are signal. This gives an upper limit of 2.3 events for $\bar{B}^0 \to \omega\gamma$, and 3.89 events for $B^- \to \rho^-\gamma$ and $\bar{B}^0 \to \rho^0\gamma$. To account for systematic uncertainties, we scale up all three upper limits by 20%. These uncertainties are dominated by our understanding of the efficiencies for the continuum suppression cuts (R_2, $S_\perp$, R_2', andcos θ').

To extract $|V_{td}/V_{ts}|$ we calculate an upper limit on the ratio $\Gamma(B \to (\rho,\omega)\gamma)/\Gamma(B \to K^*\gamma)$, where $\Gamma(B \to (\rho,\omega)\gamma)$ refers to the proper sum of partial decay widths. For B^- decays $\Gamma(B \to (\rho,\omega)\gamma)$ is simply the branching ratio to ρ^-. To calculate $\Gamma(B^0 \to (\rho,\omega))$ we sum the efficiencies for $B^- \to \rho^-\gamma$ and $\bar{B}^0 \to \omega\gamma$ with an additional factor of 1/2 to account for the quark content. In this way, we determine the efficiency for $B \to (\rho,\omega)\gamma$ to be 21.2%,

TABLE II. Constraints on $|V_{td}/V_{ts}|$

Reference	Model	ξ	Upper Limit $\lvert V_{td}/V_{ts}\rvert$
Ali *et al.* [3]	QCD Sum Rule	0.58	< 0.76
Soares [9]	BSW Formalism	0.81	< 0.64
Narison [10]	Hybrid QCD Sum Rule	0.77	< 0.66

while the efficiency for $B \to K^*\gamma$ is 17.0%.

Since the total number of events seen in the signal region for both modes is small (2 and 13), we use a binomial likelihood method to determine the upper limit on the ratio, R=N/M. N is the number of $B \to (\rho,\omega)\gamma$ events we expect to see based on the actual branching fraction and M is the same quantity for $B \to K^*\gamma$. We do not *a priori* know N and M, but we have measured n, m, B_n, and B_m where n and m are the measured number of events in the signal region for $B \to (\rho,\omega)\gamma$ and $B \to K^*\gamma$ respectively, and B_m and B_n are the expected backgrounds. The probability that we would measure n and m if the true ratio is R, is given by

$$L(R) = \frac{e^{-(B_m+B_n)}}{n!m!}\sum_{i=0}^{m}\sum_{j=0}^{n}\binom{m}{i}\binom{n}{j}(j+i+1)!B_m^{(m-i)}B_n^{(n-j)}\frac{R^j}{(R+1)^{(j+i+2)}} \qquad (2)$$

The 90% confidence level upper bound on the ratio, $R_{90\%}$, is the value for which 90% of the area of L(R) lies at smaller R. To be conservative in accounting for systematics in our background estimates, we set B_n=0 and add to B_m the sum of the uncertainties on the three $B \to K^*\gamma$ background estimates. Using the values $n = 2$, $m = 13$, $B_n = 0$, B_m =2.5 we find that $R_{90\%}$=0.55. Combining this with the ratio of efficiencies (0.80) and luminosities (0.675) between $B \to K^*\gamma$ and $B \to (\rho,\omega)\gamma$, and an 8% systematic uncertainty gives the upper limit

$$\frac{\mathcal{B}(B \to (\rho,\omega)\gamma)}{\mathcal{B}(B \to K^*\gamma)} < 0.34 \ (90\%\ \mathrm{CL})$$

The systematics on the ratio are less than the systematics on each individual mode since the uncertainties due to the continuum suppression cuts are the same for the $B \to K^*\gamma$ and the $B \to (\rho,\omega)\gamma$ analyses and therefore cancel in the ratio.

To extract $|V_{td}/V_{ts}|$ from the ratio of branching fractions we use equation (1). The phase space factor is $\Omega = 1.02 \pm 0.02$. [8] There is some range in the theoretical estimates of the SU(3) symmetry breaking which determines ξ. Table II summarizes some of the theoretical predictions for ξ and the corresponding upper limit of $|V_{td}/V_{ts}|$ for each prediction.

ALEPH has recently set an upper limit on $|V_{td}/V_{ts}|$ using the oscillations seen in the $B_d^0\bar{B}_d^0$ and $B_s^0\bar{B}_s^0$ system [11]. They give a limit of $|V_{td}/V_{ts}| < 0.63$ which is consistent with our limit. From unitarity constraints of the Kobayashi-Maskawa matrix, the ratio is bounded by $0.11 < |V_{td}/V_{ts}| < 0.35$ [12].

In conclusion, we have searched for three new FCNC electromagnetic penguin decays and have placed upper limits on these decay channels. These limits are still above the values expected from theory: $\mathcal{B}(B \to (\rho, \omega)\gamma) \simeq (0.4 - 7) \times 10^{-6}$ [9]. Therefore it will probably require an order of magnitude increase in the data sample before they are observed unless some non-Standard Model physics is present.

We gratefully acknowledge the effort of the CESR staff in providing us with excellent luminosity and running conditions. This work was supported by the National Science Foundation, the U.S. Dept. of Energy, the Heisenberg Foundation, the SSC Fellowship program of TNRLC, Natural Sciences and Engineering Research Council of Canada, and the A.P. Sloan Foundation.

REFERENCES

[1] R. Ammar, *et. al.* (CLEO), Phys. Rev. Lett. **71**, 674 (1993).

[2] Private communication from Sandip Pakvasa.

[3] A. Ali, V.M. Braun, and H. Simma, CERN Report no. CERN-Th.7118/93.

[4] G. Fox and S. Wolfram, Phys. Rev. Lett. **41**, 1581 (1978).

[5] Rumelhart D.E. and McClelland J.L., *Parallel Distributed Processing*, Vol. **1–2** (Bradford Books, MIT Press, Cambridge, MA) 1986.

[6] Minsky M.L. and Papert S., *Perceptrons: an Introduction to Computational Geometry* (exp. ed.) (MIT Press, Cambridge, MA) 1986.

[7] The results of Ref. [1] are based on 1377 pb^{-1} of integrated luminosity on the $\Upsilon(4S)$ and 633 pb^{-1} below the $\Upsilon(4S)$.

[8] The phase space factor is

$$\Omega = \frac{(m_b^2 + m_d^2)}{(m_b^2 + m_s^2)} \frac{(m_B^2 - m_\rho^2)^3}{(m_B^2 - m_{K^*}^2)^3}$$

where we have used the quark masses $m_b = 5.0$ GeV, $m_s = 300$ MeV, and $m_d = 100$ MeV. [3]

[9] J.M. Soares, Phys. Rev. D **49**, 283 (1994). The number is obtained using the Bauer-Stech-Wirbel model.

[10] S. Narison, Phys. Lett. B **327**, 354 (1994).

[11] ALEPH Collab., D. Buskulic *et al.*, Phys. Lett. B **322** 441 (1994).

[12] K. Kleinknecht and B. Renk (private communication) based on data from F.J. Gilman, K. Kleinknecht, and B. Renk, SSC Laboratory Report No. SSCL-597 Rev.1 (to be published in the 1994 Review of Particle Properties of Particle Data Group).
A. Ali and D. London, CERN Report No. CERN-TH. 7248/94 report $0.12 < |V_{td}/V_{ts}| < 0.34$ using a different method.

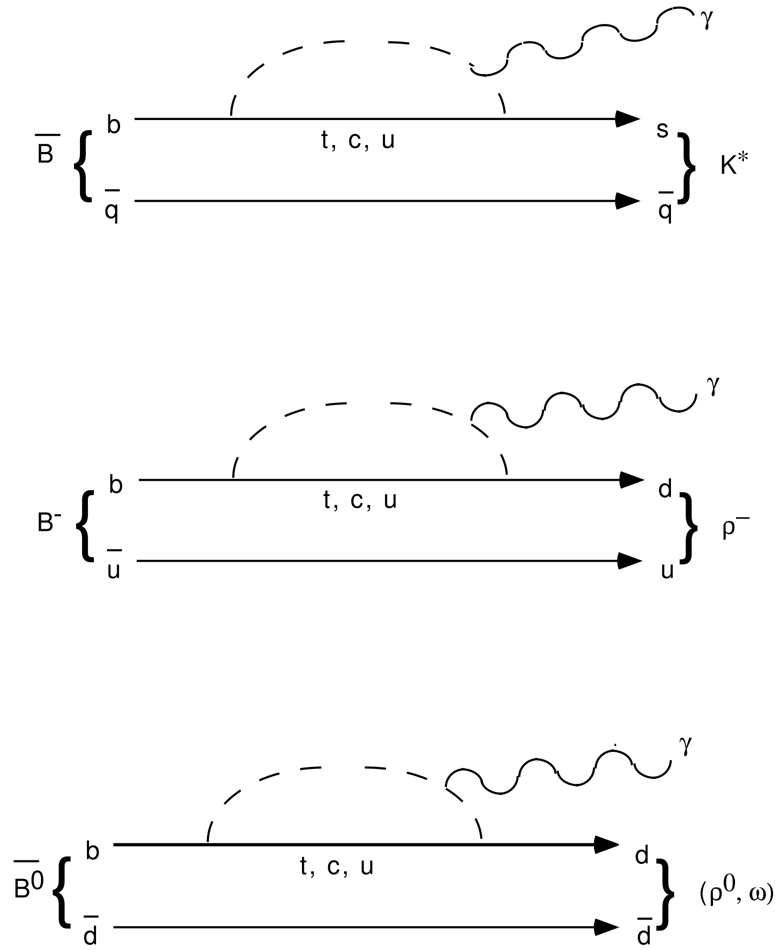

FIG. 1. Feynman diagrams of the decays $B \to K^*\gamma$, $B^- \to \rho^-\gamma$, $\bar{B}^0 \to \omega\gamma$, and $\bar{B}^0 \to \rho^0\gamma$.

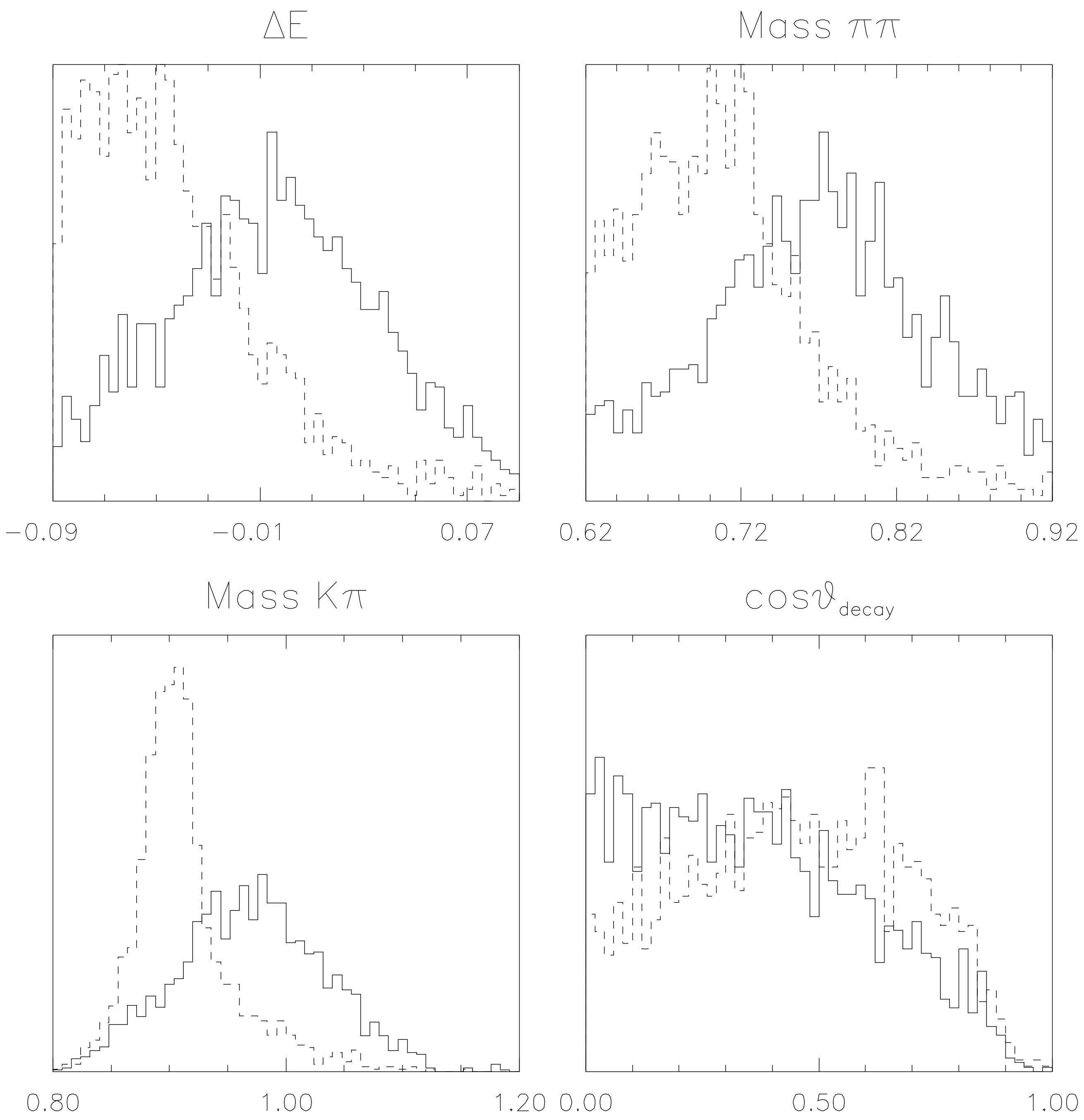

FIG. 2. The neural network inputs are shown where the $\bar{B}^0 \to \rho^0\gamma$ MC events are the solid lines and $\bar{B}^0 \to \bar{K}^{*0}\gamma$ MC events are the dashed lines.

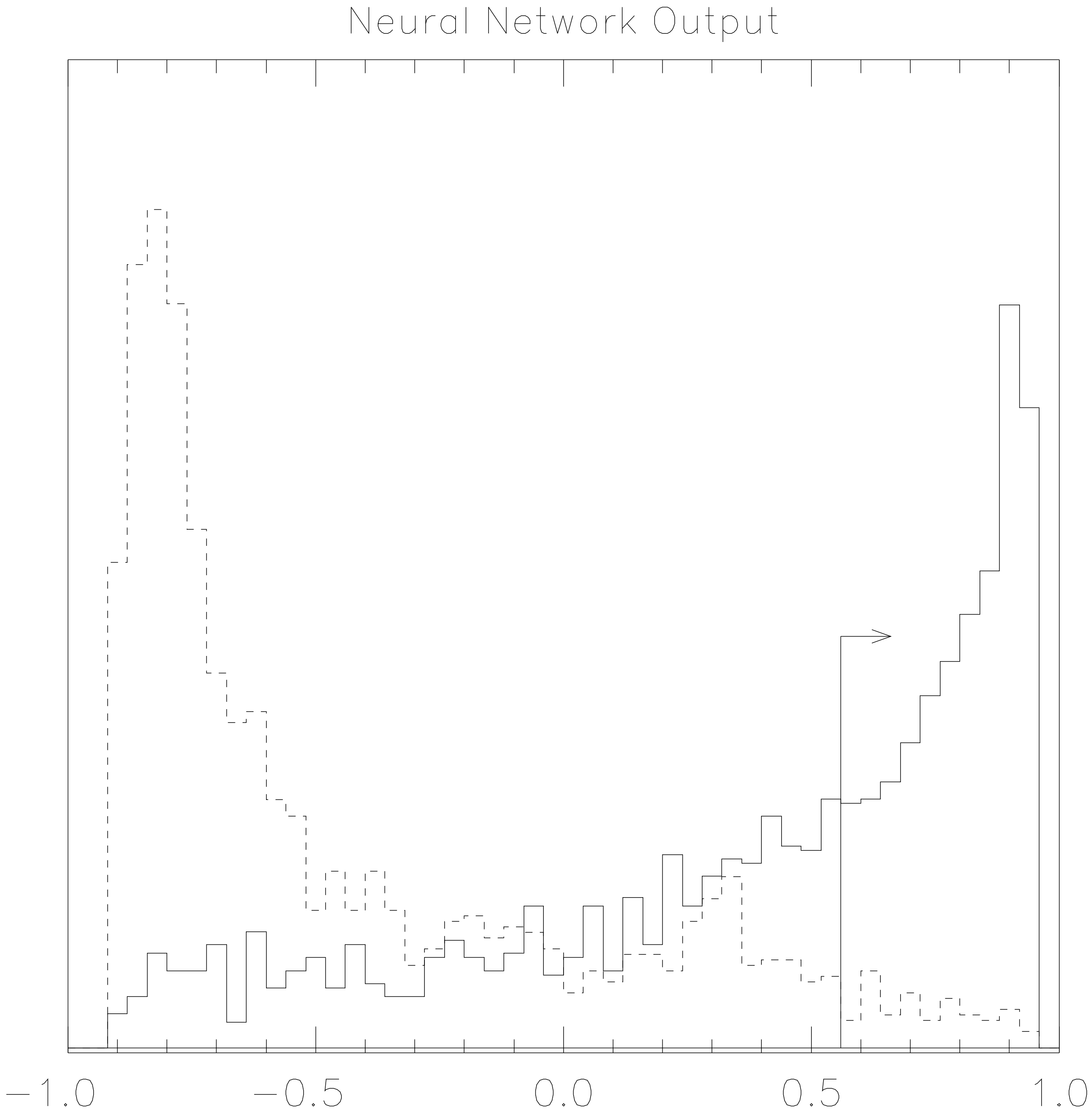

FIG. 3. The neural network output is shown with $\bar{B}^0 \to \rho^0\gamma$ in solid line and $\bar{B}^0 \to \bar{K}^{*0}\gamma$ in dashed line. The vertical line with the arrow shows the position of the cut at 0.56.

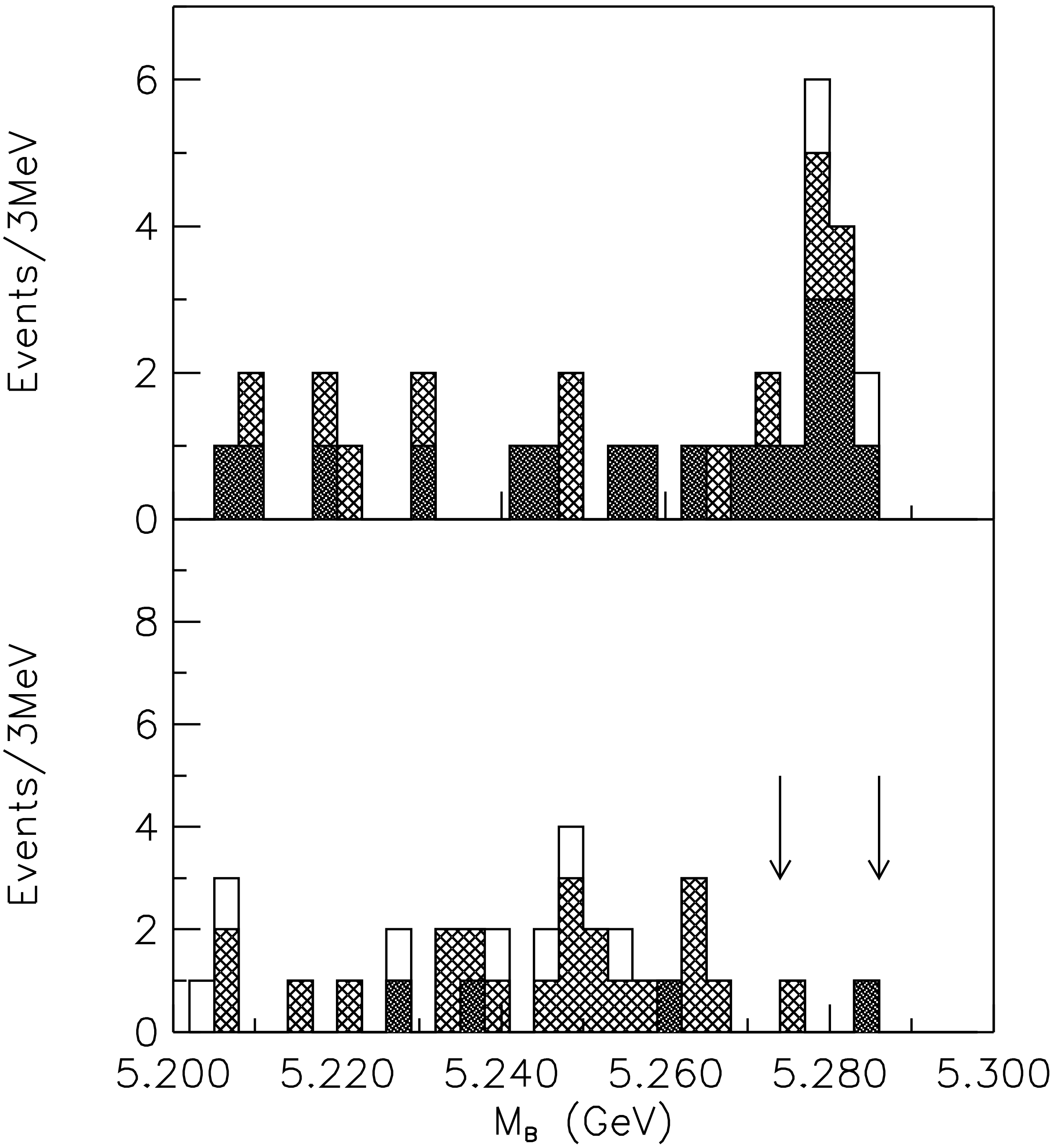

FIG. 4. The mass distributions for the B candidates for the summed $B \to K^*\gamma$ (top)[1] and $B \to (\rho,\omega)\gamma$ (bottom). The $B \to (\rho,\omega)\gamma$ plot includes 50% more luminosity than the $B \to K^*\gamma$ plot. The arrows indicate the signal region defined as $5.274 < M_B < 5.286$ GeV. The dark entries for the upper (lower) plot are the $K^-\pi^+\gamma$ ($\rho^0\gamma$) events, the cross-hatched $K^-\pi^0\gamma$ ($\rho^-\gamma$), and the white $K^0_S\pi^-\gamma$ ($\omega\gamma$).